EGFR MUTATIONS AND CELL TYPES IN LUNG ADENOCARCINOMAS

Cell type classification of lung adenocarcinomas was originally performed by Hashimoto et al,[37] describing hobnail, columnar, polygonal, goblet, and mixed cell types. They combined the Clara (nonciliated bronchiolar) cell type and type II cell type as the hobnail cell type because these types have the same cytologic features and are usually found to be mixed. This classification was applied with slight modification to a series of lesions in our hospitals. We divided lung cancers into hobnail, columnar, and polygonal cell types, focusing on the most frequent cell type rather than using the mixed cell category. Also, we merged the goblet and columnar cell types because of similarity in histologic and etiologic features and because the goblet cell type is present in minority (Figure 4, A through C).

As a result, the hobnail cell type was found to be significantly more associated with EGFR mutations than any of the other groups ($P < .001$). The cell type classification also relates to differences in mutation frequency and pattern of *TP53* (which codes for p53 protein).[37] The hobnail cell type, characterized by cytoplasmic protrusions and a tadpole or hobnail appearance, shows a low *TP53* mutational frequency, mainly of spontaneous transition type at CpG nucleotides. In contrast, the columnar cell type shows a high *TP53* mutational frequency, with G to T transversions, considered to be caused by exogenous carcinogenic agents like those found in tobacco smoke. We identified a significant difference in EGFR mutation rates between the hobnail cell type and the other 2 types. This finding provided further evidence of differences in the genetic background of EGFR mutations.

EGFR MUTATIONS AND MICROPAPILLARY PATTERN OR BAC HISTOLOGY IN LUNG ADENOCARCINOMAS

Additionally, we have focused on the presence of BAC component, as well as micropapillary pattern (MPP), defined as papillary structures with tufts lacking a fibrovascular core (Figure 5, A and B).[38] The micropapillary component belongs to moderately differentiated structures because of the lack of stroma.[38] When a cancer comprises more than 5% MPP, the prognosis has been shown to be poor, even with pathologic stage I disease.[38]

As a result, there was a significant association between the existence of BAC component or MPP and EGFR mutations ($P = .01$ and $P = .04$, respectively). In addition, both BAC component and MPP were significantly associated with the hobnail cell type ($P < .001$ and $P = .01$, respectively), as compared with the combined group of columnar and polygonal cell types. However, there was no association between BAC components and MPP ($P = .75$).[36]

The MPP is a distinct pathologic subtype first reported in lung cancers by Amin et al.[39] Among early stage lung adenocarcinomas, MPP-positive cancers show a significantly poorer prognosis than those that are MPP negative.[38] We speculated that the distinct MPP feature reflects a step of tumor progression from well-differentiated papillary adenocarcinoma of the hobnail cell type to a less differentiated state, unrelated to smoking. From their pathologic presentation and relatively unfavorable outcome, it is suggested that cancers with MPP should be classified as moderately differentiated rather than well dif-

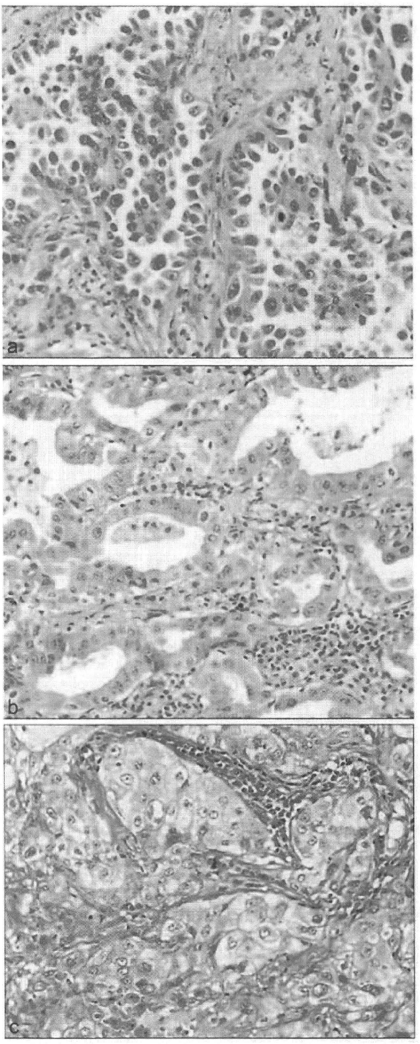

Figure 4. *Microscopic appearance of the 3 cytologic subtypes. A, Hobnail cell type. Apical portions of carcinoma cells containing nuclei protrude or bulge into the lumen. B, Columnar cell type. Nonciliated columnar or cuboidal cells, with or without mucus in their cytoplasm, have flat apical portions. C, Polygonal cell type. Note polygonal cells showing sheet-like growth (hematoxylin-eosin, original magnifications ×400).*

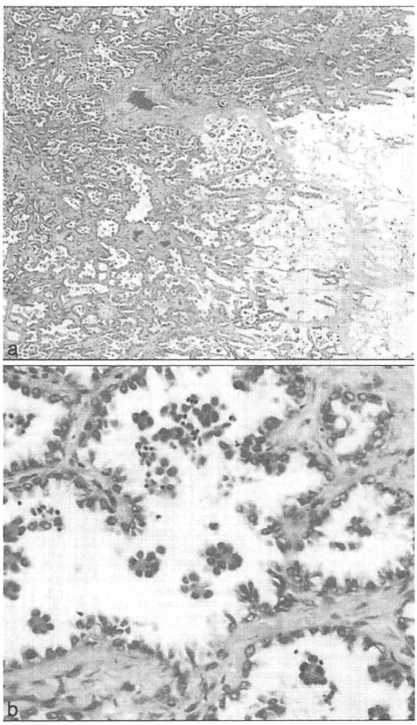

Figure 5. *Histologic features of the micropapillary pattern in pulmonary adenocarcinomas. A, Note diffuse distribution of tufts in alveolar spaces. B, Papillary tufts lack central fibrovascular cores (hematoxylin-eosin, original magnifications ×40 [A] and ×400 [B]).*

ferentiated. This pattern is often observed in nonsmokers and correlates with a high degree of tumor aggression. We also have demonstrated that metastasis to lymph nodes, pleural invasion, intrapulmonary metastases, and nonsmoking status are significantly more frequent in MPP-positive cases with a significantly poorer survival.[38] In our study, the presence of MPP components significantly correlated with EGFR mutations. Kim et al[40] referred to an association between the presence of MPP and tumor sensitivity to an EGFR TK inhibitor, although their analysis was limited to 36 relapsed lung adenocarcinomas. A notable characteristic of MPP is its frequent presence at the periphery of cancers and its predominance in metastatic foci.[39,41] These clinicopathologic observations, accompanied by our findings of a high mutational frequency for EGFR, may explain the dramatic responses to gefitinib in lung adenocarcinomas with diffuse micronodular intrapulmonary metastasis.[42]

COMMENT ON EGFR MUTATIONS AND CLINICOPATHOLOGIC FEATURES

Both BAC components and MPP are prevalent among nonsmokers.[38,43] Considering the etiologic relevance and its correlation with EGFR mutations, we speculate that lung cancers with these features belong to the same lineage characterized by thyroid transcription factor–1[35] and the hobnail cell type. Also, the results imply that lesions featuring MPP may be at a slightly more advanced stage than those with BAC components, because the MPP is an adverse prognostic marker for pathologic stage I disease.[38] Lung cancers in nonsmokers are considered to be less genetically complex than those in smokers[44,45] and, therefore, they may have distinct characteristics depending on simple signaling pathways, such as EGFR/Akt, for maintenance and survival.[2] Consequently, patients with tumors harboring these pathologic features could be good candidates and benefit from EGFR TK inhibitors.

CONCLUSION

There is no doubt that the EGFR TK inhibitors and EGFR monoclonal antibodies offer innovative molecular-targeted drugs, effective for some NSCLCs. However, the possibility of acute lung damage and interstitial pneumonia as negative side effects must be borne in mind. Therefore, the fact that in patients who are young, female, never-smokers, and of East Asian ethnicity, one subtype of NSCLC positively responds to EGFR TK inhibitors—because of the presence of EGFR mutations—is of great importance.

Pathologically, the hobnail cell type, MPP, and BAC components of lung adenocarcinomas are associated with a high incidence of EGFR mutations. Adenocarcinomas with these features form a distinct subtype, a fact suggesting that a genetic background confers susceptibility to EGFR TK inhibitors. The immunohistochemical analysis has a potential vulnerability because different antibodies might yield different results. Hence, these histologic features of lung adenocarcinomas with EGFR mutations, which can be detected by hematoxylin-eosin staining, are meaningful. These findings could provide a clue for selection of patients who might benefit from such treatment, as well as insights into biologic mechanisms of phenotype-genotype correlations.

Parts of this study were supported financially by Grants-in-Aid for Scientific Research from the Ministry of Education, Culture, Sports, Science and Technology of the Japan Society for the Promotion of Science and by grants from the Ministry of Health, Labour and Welfare, the Smoking Research Foundation, the National Institute of Biomedical Innovation, and the Vehicle Racing Commemorative Foundation, as well as a Grant-in-Aid for Young Scientists (B).

References

1. Lynch TJ, Bell DW, Sordella R, et al. Activating mutations in the epidermal growth factor receptor underlying responsiveness of non-small-cell lung cancer to gefitinib. *N Engl J Med.* 2004;350:2129–2139.

2. Paez JG, Janne PA, Lee JC, et al. EGFR mutations in lung cancer: correlation with clinical response to gefitinib therapy. *Science.* 2004;304:1497–1500.

3. Pao W, Miller V, Zakowski M, et al. EGF receptor gene mutations are common in lung cancers from "never smokers" and are associated with sensitivity of tumors to gefitinib and erlotinib. *Proc Natl Acad Sci U S A.* 2004;101:13306–13311.

4. Shigematsu H, Lin L, Takahashi T, et al. Clinical and biological features associated with epidermal growth factor receptor gene mutations in lung cancers. *J Natl Cancer Inst.* 2005;97:339–346.

5. Mitsudomi T, Viallet J, Mulshine JL, Linnoila RI, Minna JD, Gazdar AF. Mutations of ras genes distinguish a subset of non-small-cell lung cancer cell lines from small-cell lung cancer cell lines. *Oncogene.* 1991;6:1353–1362.

6. Soda M, Choi YL, Enomoto M, et al. Identification of the transforming EML4-ALK fusion gene in non-small-cell lung cancer. *Nature.* 2007;448:561–566.

7. Kosaka T, Yatabe Y, Endoh H, Kuwano H, Takahashi T, Mitsudomi T. Mutations of the epidermal growth factor receptor gene in lung cancer: biological and clinical implications. *Cancer Res.* 2004;64:8919–8923.

8. Inamura K, Takeuchi K, Togashi Y, et al. EML4-ALK fusion is linked to histological characteristics in a subset of lung cancers. *J Thorac Oncol.* 2008;3:13–17.

9. Carpenter G, Lembach KJ, Morrison MM, Cohen S. Characterization of the binding of 125-I-labeled epidermal growth factor to human fibroblasts. *J Biol Chem.* 1975;250:4297–4304.

10. Carpenter G, King L Jr, Cohen S. Epidermal growth factor stimulates phosphorylation in membrane preparations in vitro. *Nature.* 1978;276:409–410.

11. Downward J, Yarden Y, Mayes E, et al. Close similarity of epidermal growth factor receptor and v-erb-B oncogene protein sequences. *Nature.* 1984;307:521–527.

12. Herbst RS, Shin DM. Monoclonal antibodies to target epidermal growth factor receptor-positive tumors: a new paradigm for cancer therapy. *Cancer.* 2002; 94:1593–1611.

13. Kimura M, Tsuda H, Morita D, et al. A proposal for diagnostically meaningful criteria to classify increased epidermal growth factor receptor and c-erbB-2 gene copy numbers in gastric carcinoma, based on correlation of fluorescence in situ hybridization and immunohistochemical measurements. *Virchows Arch.* 2004;445:255–262.

14. Kimura M, Tsuda H, Morita D, et al. Usefulness and limitation of multiple endoscopic biopsy sampling for epidermal growth factor receptor and c-erbB-2 testing in patients with gastric adenocarcinoma. *Jpn J Clin Oncol.* 2005;35:324–331.

15. Ueda S, Ogata S, Tsuda H, et al. The correlation between cytoplasmic overexpression of epidermal growth factor receptor and tumor aggressiveness: poor prognosis in patients with pancreatic ductal adenocarcinoma. *Pancreas.* 2004;29:e1–e8.

16. Ueda S, Hatsuse K, Tsuda H, et al. Potential crosstalk between insulin-like growth factor receptor type 1 and epidermal growth factor receptor in progression and metastasis of pancreatic cancer. *Mod Pathol.* 2006;19:788–796.

17. Murakawa T, Tsuda H, Tanimoto T, Tanabe T, Kitahara S, Matsubara O. Expression of KIT, EGFR, HER-2 and tyrosine phosphorylation in undifferentiated thyroid carcinoma: implication for a new therapeutic approach. *Pathol Int.* 2005; 55:757–765.

18. Nicholson RI, Gee JM, Harper ME. EGFR and cancer prognosis. *Eur J Cancer.* 2001;37(suppl 4):S9–S15.

19. Yamazaki H, Fukui Y, Ueyama Y, et al. Amplification of the structurally and functionally altered epidermal growth factor receptor gene (c-erbB) in human brain tumors. *Mol Cell Biol.* 1988;8:1816–1820.

20. Batra SK, Castelino-Prabhu S, Wikstrand CJ, et al. Epidermal growth factor ligand-independent, unregulated, cell-transforming potential of a naturally occurring human mutant EGFRvIII gene. *Cell Growth Differ.* 1995;6:1251–1259.

21. Pedersen MW, Meltorn M, Damstrup L, Poulsen HS. The type III epidermal growth factor receptor mutation: biological significance and potential target for anti-cancer therapy. *Ann Oncol.* 2001;12:745–760.

22. Kosaka T, Endoh H, Yatabe Y, Mitsudomi T. Translational research on lung cancer—EGFR gene mutation [in Japanese]. *Gan To Kagaku Ryoho.* 2005;32: 750–758.

23. Choi SH, Mendrola JM, Lemmon MA. EGF-independent activation of cell-surface EGF receptors harboring mutations found in gefitinib-sensitive lung cancer. *Oncogene.* 2007;26:1567–1576.

24. Tang X, Shigematsu H, Bekele BN, et al. EGFR tyrosine kinase domain mutations are detected in histologically normal respiratory epithelium in lung cancer patients. *Cancer Res.* 2005;65:7568–7572.

25. Ji H, Li D, Chen L, et al. The impact of human EGFR kinase domain mutations on lung tumorigenesis and in vivo sensitivity to EGFR-targeted therapies. *Cancer Cell.* 2006;9:485–495.

26. Balak MN, Gong Y, Riely GJ, et al. Novel D761Y and common secondary T790M mutations in epidermal growth factor receptor-mutant lung adenocarcinomas with acquired resistance to kinase inhibitors. *Clin Cancer Res.* 2006;12: 6494–6501.

27. Fukuoka M, Yano S, Giaccone G, et al. Multi-institutional randomized phase II trial of gefitinib for previously treated patients with advanced non-small-cell lung cancer (The IDEAL 1 Trial) [corrected]. *J Clin Oncol.* 2003;21:2237–2246.

28. Kris MG, Natale RB, Herbst RS, et al. Efficacy of gefitinib, an inhibitor of the epidermal growth factor receptor tyrosine kinase, in symptomatic patients with non-small cell lung cancer: a randomized trial. *JAMA.* 2003;290:2149–2158.

29. Giaccone G, Herbst RS, Manegold C, et al. Gefitinib in combination with gemcitabine and cisplatin in advanced non-small-cell lung cancer: a phase III trial—INTACT 1. *J Clin Oncol.* 2004;22:777–784.

30. Herbst RS, Giaccone G, Schiller JH, et al. Gefitinib in combination with paclitaxel and carboplatin in advanced non-small-cell lung cancer: a phase III trial—INTACT 2. *J Clin Oncol.* 2004;22:785–794.

31. Thatcher N, Chang A, Parikh P, et al. Gefitinib plus best supportive care in previously treated patients with refractory advanced non-small-cell lung cancer: results from a randomised, placebo-controlled, multicentre study (Iressa Survival Evaluation in Lung Cancer). *Lancet.* 2005;366:1527–1537.

32. Inoue A, Saijo Y, Maemondo M, et al. Severe acute interstitial pneumonia and gefitinib. *Lancet.* 2003;361:137–139.

33. Miller VA, Kris MG, Shah N, et al. Bronchioloalveolar pathologic subtype and smoking history predict sensitivity to gefitinib in advanced non-small-cell lung cancer. *J Clin Oncol.* 2004;22:1103–1109.

34. Hsieh RK, Lim KH, Kuo HT, Tzen CY, Huang MJ. Female sex and bronchioloalveolar pathologic subtype predict EGFR mutations in non-small cell lung cancer. *Chest.* 2005;128:317–321.

35. Yatabe Y, Kosaka T, Takahashi T, Mitsudomi T. EGFR mutation is specific for terminal respiratory unit type adenocarcinoma. *Am J Surg Pathol.* 2005;29: 633–639.

36. Ninomiya H, Hiramatsu M, Inamura K, et al. Correlation between morphology and EGFR mutations in lung adenocarcinomas: significance of the micropapillary pattern and the hobnail cell type. *Lung Cancer.* 2009;63:235–240.

37. Hashimoto T, Tokuchi Y, Hayashi M, et al. Different subtypes of human lung adenocarcinoma caused by different etiological factors: evidence from p53 mutational spectra. *Am J Pathol.* 2000;157:2133–2141.

38. Miyoshi T, Satoh Y, Okumura S, et al. Early-stage lung adenocarcinomas with a micropapillary pattern, a distinct pathologic marker for a significantly poor prognosis. *Am J Surg Pathol.* 2003;27:101–109.

39. Amin MB, Tamboli P, Merchant SH, et al. Micropapillary component in lung adenocarcinoma: a distinctive histologic feature with possible prognostic significance. *Am J Surg Pathol.* 2002;26:358–364.

40. Kim YH, Ishii G, Goto K, et al. Dominant papillary subtype is a significant predictor of the response to gefitinib in adenocarcinoma of the lung. *Clin Cancer Res.* 2004;10:7311–7317.

41. Makimoto Y, Nabeshima K, Iwasaki H, et al. Micropapillary pattern: a distinct pathological marker to subclassify tumours with a significantly poor prognosis within small peripheral lung adenocarcinoma (</=20 mm) with mixed bronchioloalveolar and invasive subtypes (Noguchi's type C tumours). *Histopathology.* 2005;46:677–684.

42. Kobayashi M, Takeuchi T, Bandobashi K, et al. Diffuse micronodular pulmonary metastasis of lung adenocarcinoma predicts gefitinib response in association with epidermal growth factor receptor mutations. *Anticancer Res.* 2006; 26:1621–1626.

43. Okubo K, Mark EJ, Flieder D, et al. Bronchoalveolar carcinoma: clinical, radiologic, and pathologic factors and survival. *J Thorac Cardiovasc Surg.* 1999; 118:702–709.

44. Sanchez-Cespedes M, Ahrendt SA, Piantadosi S, et al. Chromosomal alterations in lung adenocarcinoma from smokers and nonsmokers. *Cancer Res.* 2001;61:1309–1313.

45. Powell CA, Bueno R, Borczuk AC, et al. Patterns of allelic loss differ in lung adenocarcinomas of smokers and nonsmokers. *Lung Cancer.* 2003;39:23–29.

and neoplasia. The inflammatory cell infiltrate present in the foci of the gastric metaplastic epithelium in lieu of the bronchial mucosa favors this hypothesis.

References

1. Marty-Ane CH, Prudhome M, Fabre JM, Domergue J, Balmes M, Mary H. Tracheoesophagogastric anastomosis fistula: a rare complication of esophagectomy. *Ann Thorac Surg.* 1995;60:690-3.
2. Hendren WG, Miller JI. Isolated, contained esophagobronchial fistula complicating esophagogastrectomy. *Ann Thorac Surg.* 1988;46:457-8.
3. Piessen G, Lamblin A, Triboulet JP, Mariette C. Peptic ulcer of the gastric tube after esophagectomy for cancer: clinical implications. *Dis Esophagus.* 2007;20:542-5.
4. Stal JM, Hanly PJ, Darling GE. Gastrobronchial fistula: an unusual complication of esophagectomy. *Ann Thorac Surg.* 1994;58:886-7.
5. Bona D, Sarli D, Saino G, Quarenghi M, Bonavina L. Successful conservative management of benign gastro-bronchial fistula after intrathoracic esophagogastrostomy. *Ann Thorac Surg.* 2007;84:1036-8.

Primary pulmonary meningioma: Ten-year follow-up findings for a multiple case, implying a benign biological nature

Yukitoshi Satoh[a,b] and Yuichi Ishikawa,[a] Tokyo and Kanagawa, Japan

In 1998 we[1] reported the first case of multiple pulmonary meningioma, an extremely uncommon lung neoplasm. To date, there have been only 30 cases of primary pulmonary meningioma (PPM) reported in the English literature.[1-3] Although the lesions are widely known to be usually benign, slow growing, and to have an excellent prognosis, the etiology is still uncertain. Hence, several mechanisms have been proposed.[1,3,4] We here report the clinical course of the initial case 10 years after surgery with examination by different imaging modalities and additional biopsy findings for a metachronous pulmonary lesion.

CLINICAL SUMMARY

A 74-year-old Japanese woman with a history of multiple PPM, undergoing surgery for lesions at the age of 64, was followed up by chest computed tomographic (CT) scan and magnetic resonance imaging (MRI) thereafter. During this period the patient was once referred to the Cancer Institute Hospital for percutaneous biopsy and cytologic examination of a new asymptomatic nodule that appeared in the right lower lung field 10 years after the first surgical resection (Figure 1). Histologic examination of the nodule revealed a benign PPM, which showed the same features as the lesion reported previously (Figure 2). Immunohistochemical staining performed by a standard avidin–biotin immunoperoxidase technique demonstrated consistent expression of epithelial membrane antigen and vimentin in tumor cells. Conversely, results of studies for S-100 protein, AE1/AE3, CAM 5.2, muscle-specific actin (HHF-35), smooth muscle actin, synptophysin neuron-specific antigen, and desmin were negative. Furthermore, the tumor cells were focally positive for CD68 by KP-1 and progesterone receptor. Cytologic examination also demonstrated meningioma features, as for the lesion reported previously.[1]

MRI of the brain showed no abnormalities, and no intracranial or intraspinal masses were identified. On the basis of the morphologic features and the benign clinical course, the patient is being followed up by CT scan with informed consent. Although the right lung nodule has grown, the growth is very slow with a doubling time of 1011 days, the patient is asymptomatic, and there are no other new lesions in the lungs.

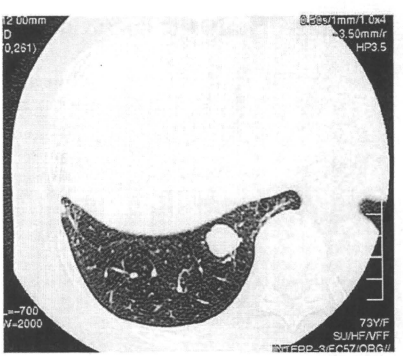

FIGURE 1. Chest computed tomographic scan showing a nodule in the right lower lung field.

From the Department of Pathology,[a] Cancer Institute, Japanese Foundation for Cancer Research, Tokyo, and the Department of Thoracic Surgery,[b] Kitasato University School of Medicine, Kanagawa, Japan.

Disclosures: None.

Received for publication May 31, 2008; revisions received June 25, 2008; accepted for publication July 6, 2008; available ahead of print Dec 22, 2008.

Address for reprints: Yukitoshi Satoh, MD, Kitasato University School of Medicine, Department of Thoracic Surgery, 1-15-1 kitasato, Sagamihara-shi Kanagawa, 228-8555 Japan (E-mail: ysatoh@med.kitasato-u.ac.jp).

J Thorac Cardiovasc Surg 2010;139:e39-40
0022-5223/$36.00

doi:10.1016/j.jtcvs.2008.07.059

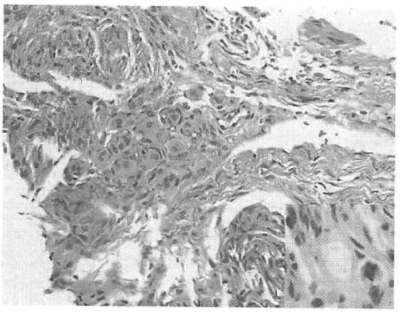

FIGURE 2. Microscopically, the nodule consists of tumor cells demonstrating a mixture of meningotheliomatous and fibrous elements (hematoxylin and eosin stain). A psammoma body is evident (islet).

DISCUSSION

We have successfully followed up the first case of multiple pulmonary meningioma by CT scan for more than 10 years after the first operation. During this period, the possibility of metastasis from an intracranial or intraspinal primary tumor was excluded by imaging modalities including CT scan and MRI. Another lesion developed in the right lung and was histologically confirmed to be meningioma, but increase in size was very slow and the lesion has remained solitary.

Immunohistochemically, the findings supported a meningothelial origin for the lesion, in line with other reports.[1,3] The exact origin of meningiomas in the thorax is still debated, and different theories have been advocated, such as intrathoracic differentiation of meningocytes or arachnoid cells, ectopic proliferation of arachnoid cells, or direct/indirect extension of primary intracranial meningiomas.[1-4] In the present case, the following possibility may explain the synchronous and metachronous multiplicity: multiple pulmonary meningothelium-like nodules grew synchronously and metachronously.[1,5] The tumor usually grows very slowly and patients are often free of symptoms. Even though the majority of cases demonstrate a benign behavior, the treatment usually consists of complete surgical resection. In the present case, although the new lesion demonstrated continued growth on imaging, a benign native lesion was evident on the basis of examination of a percutaneous biopsy specimen. Thus, we concluded that these tumors are amenable to surgical resection, especially in cases that prove to be benign by biopsy or cytologic examination.

References

1. Ueno M, Fujiyama J, Uchiyama T, Ishikawa Y, Satoh Y. Cytology of primary pulmonary meningioma: report of the first multiple case. *Acta Cytol.* 1998;42:1424-30.
2. Meirelles GS, Ravizzini G, Moreira AL, Akhurst T. Primary pulmonary meningioma manifesting as a solitary pulmonary nodule with a false-positive PET scan. *J Thorac Imaging.* 2006;21:225-7.
3. Comin CE, Caldarella A, Novelli L, Janni A. Primary pulmonary meningioma: report of a case and review of the literature. *Tumori.* 2003;89:102-5.
4. Lockett L, Chiang V, Scully N. Primary pulmonary meningioma. Report of a case and review of the literature. *Am J Surg Pathol.* 1997;21:453-60.
5. Suster S, Moran CA. Diffuse pulmonary meningotheliomatosis. *Am J Surg Pathol.* 2007;31:624-31.

Angiosarcoma in the aortic arch presented as repeat strokes

Yu-Yun Nan, MD,[a] Yuan-Chang Liu, MD,[b] Ming-Shian Lu, MD,[a] Sui Hsueh, MD,[c] Hsien-Kun Chang, MD,[d] and Yao-Kuang Huang, MD,[a,e] Linkou, Chia-Yi, and Taipei, Taiwan

From the Division of Thoracic and Cardiovascular Surgery[a] and the Departments of Medial Image and Intervention,[b] Pathology,[c] and Oncology,[d] Chang Gung Memorial Hospital, and Chang Gung University, College of Medicine, Linkou and Chia-Yi, Taiwan, and the Graduate Institute of Clinical Medicines,[e] College of Medicine, Taipei Medical University, Taipei, Taiwan.

Disclosures: None.

Received for publication Aug 28, 2008; revisions received Sept 28, 2008; accepted for publication Oct 16, 2008; available ahead of print Feb 23, 2009.

Address for reprints: Yao-Kuang Huang, MD, Division of Cardiac Surgery, Chang Gung Memorial Hospital, Linkou, and Graduate Institute of Clinical Medicine, College of Medicine, Taipei Medical University, 5, Fu-Shin Rd, Kwei-Shan, Taoyuan, Taiwan 33377 (E-mail: huang137@mac.com).

J Thorac Cardiovasc Surg 2010;139:e40-2

0022-5223/$36.00

doi:10.1016/j.jtcvs.2008.10.020

A 51-year-old man visited a local medical clinic 4 weeks before admission because of a 6-month history of weight loss and anorexia. His medical history was unremarkable except for a blood pressure discrepancy in both arms on physical examination. Furthermore, a palpable abdominal mass was found and proved later to be a probable malignant adrenal tumor by means of abdominal computed tomographic analysis.

He experienced several episodes of unconsciousness with cyanotic apnea, which required brief resuscitation and mechanical ventilator support. An unusual mass inside the innominate artery was discovered in a brain computed

Discriminant Model for Cytologic Distinction of Large Cell Neuroendocrine Carcinoma from Small Cell Carcinoma of the Lung

Rira Hoshi, CT, Noriyuki Furuta, CT,* Takeshi Horai, MD,* Yuichi Ishikawa, MD, PhD,† Satoshi Miyata, PhD,‡ and Yukitoshi Satoh, MD, PhD*§*

Background: To establish cytologic criteria for pulmonary large cell neuroendocrine carcinoma (LCNEC), we developed and evaluated a discriminant model for cytologic differential diagnosis between LCNEC and small cell lung carcinoma (SCLC).

Methods: Aspiration cytologic and/or imprint smears from 29 LCNEC cases were reviewed in comparison with 26 SCLC cases. We selected the following parameters for assessment: background, cellular arrangement, cell clusters, cell cohesion, arrangements, cell dimensions areas, the presence of cytoplasm and/or prominent nucleoli, nuclear features, mitosis, naked nuclei, and nuclear streaking. To demonstrate the utility of differences in frequencies of cytologic parameters for LCNECs and SCLCs, a discriminant model was developed and evaluated.

Results: Among the cytologic parameters investigated, large clusters (consisting of ≥60 tumor cells) with tight cohesion and small tumor cells (showing ≤120 μm^2) without prominent nucleoli on each case were particular focuses of attention, because statistically significant differences with good power were evident between the LCNEC and SCLC groups for their frequencies ($p < 0.0001$). On the basis of variation in plotted location on scatter plots, a discriminant model for LCNEC and SCLC was made and evaluated by logistic discriminant analysis. Sensitivity, specificity, and accuracy were all 100%. With leave-one-out cross validation, the predicted error rate of the discriminant model for new cases was 0.00545.

Conclusion: Our model based on the cytologic features of large cell clusters with tight cohesion and of small tumor cells without prominent nucleoli should be a useful aid for distinction between LCNECs and SCLCs.

From the *Departments of Cytology, Cancer Institute Hospital, Japanese Foundation of Cancer Research, Tokyo, Japan; †Department of Pathology, and ‡Bioinformatics Group, Genome Center, the Cancer Institute, the Japanese Foundation for Cancer Research, Tokyo, Japan; and §Department of Thoracic Surgery, Kitasato University School of Medicine, Kanagawa, Japan.

Disclosure: The authors declare no conflicts of interest.

Address for correspondence: Yukitoshi Satoh, MD, PhD, Department of Thoracic Surgery, Kitasato University School of Medicine, 1-15-1 Kitasato, Sagamihara-shi, Kanagawa 228-8555, Japan. Email: ysatoh@med.kitasato-u.ac.jp

ISSN: 1556-0864/10/0504-0472

Key Words: Lung cancer, Large cell neuroendocrine carcinoma, Small cell lung carcinoma, Discriminant model, Cytology.

(*J Thorac Oncol.* 2010;5: 472–478)

Large cell neuroendocrine carcinoma (LCNEC) of the lung and small cell lung carcinoma (SCLC) are both now considered as high-grade neuroendocrine carcinomas arising in the lung.[1–4] Based on the large, multiinstitutional study in Japan, Asamura et al.[5] reported that the 5-year survival rates of patients with all stages were 40.3% for LCNEC and 35.7% for SCLC, the differenc not being statistically significant. However, these two tumors are generally thought to have different clinical features[1,4,6–14] and require different treatments.

Currently, surgical resection is advocated for the LCNEC as same as other nonsmall cell lung cancers.[15] However, Iyoda et al.[10] reported that patients with stage I disease treated with either neoadjuvant or postoperative adjuvant chemotherapy had a significantly better prognosis than their counterparts groups receiving surgery alone. Therefore, LCNEC requires a refined histology-specific approach. Conversely, the SCLC is aggressive but chemosensitive, and a standard therapeutic strategy has already been established.[5]

The cytologic diagnosis of SCLC is clear, but criteria for the LCNEC have yet to be established.[5,16–22] Recently, the cytologic features of LCNEC described in several reports are as follows: necrotic background, loose cell aggregates, large cell size (three times as large as mature lymphocytes), rosette and Indian-filing arrangements, abundant cytoplasm, granular nuclear chromatin, clear nucleoli, naked nuclei, and nuclear streaking.[17–22] Because these are also often recognized in SCLC cases,[15,16,23] they are not specific.

The aim of this study was to elucidate the cytologic characteristics of the LCNEC in comparison with SCLCs particularly and evaluate the utility of proposed scoring system for their differential diagnosis.

MATERIALS AND METHODS

Patients

The pathology files of the Cancer Institute Hospital (Tokyo, Japan) between 1990 and 2007 were searched for 29 patients who underwent pulmonary resection for LCNECs.

These LCNEC cases were all confirmed by pathologic examination on surgically resected materials with the World Health Organization (WHO) classification system.[15] The histologic diagnostic criteria of LCNEC proposed by WHO are as follows: neuroendocrine morphologic features (organoid nesting, palisading, rosettes, and trabecular growth pattern); a high mitotic rate (>10 per 10 high-power fields); necrosis (often large zones); cellular features of a nonsmall cell carcinoma (large cell size, a low nuclear/cytoplasmic ratio, polygonal shape, finely granular eosinophilic cytoplasm, coarse chromatin, and/or frequent nucleoli); and neuroendocrine features by immunohistochemistry or electron microscopy or both.[15] For comparison, we randomly extracted 26 cases of SCLCs diagnosed during the same period, 16 of which were diagnosed with surgical materials and the remaining 10 with transbronchial lung biopsy samples. The histologic diagnosis of SCLCs was also based on the WHO classification system.[15] Combined LCNECs and SCLCs and SCLC cases after any treatment were all excluded in this study, which was approved by our institutional review board, each patient giving written informed consent before treatment.

Cytologic Materials

Cytologic specimens obtained by transbronchial aspiration and/or imprint from the resected specimens were fixed routinely in 95% ethanol and stained by the Papanicolaou method. Five to 12 cytologic slides were reviewed for each patient. From previous studies,[17–22] we selected the following parameters for assessment: necrotic background, cellular arrangement, tumor cell clusters, tumor cell cohesion, cell arrangements, cell dimensions areas, the presence of tumor cells with identifiable cytoplasm and/or prominent nucleoli, nuclear features, mitosis, naked nuclei, and nuclear streaking. Cluster size was categorized in the three groups as follows: small clusters, consisting of more than 10 and less than or equal to 20 cells; intermediate-sized clusters, consisting of more than 20 cells and less than 60 cells; and large clusters, consisting of more than or equal to 60 cells. Tight cohesiveness of clusters was defined as a straight cluster border composed of cells lined up and/or arranged in palisades. Cell areas were measured for 50 cells extracted at random in each specimen and calculated as (long diameter + short diameter/ $2 \times 2)^2 \pi$ ($\pi = 3.14$). The diameters of tumor cells were measured using an ocular micrometer (DSM; Olympus, Tokyo, Japan). Cell size was categorized in 2 groups as follows: small tumor cells, less than or equal to 120 μm^2; and large tumor cells, more than or equal to 600 μm^2.

Statistical Analysis

The clinicopathologic factors analyzed in this study included age (<65 or ≥65 years), gender, and smoking habits, evaluated by the χ^2 test. Differences in cell areas and the frequency of the cytologic features between LCNEC and SCLC cases were analyzed by an unpaired Student t test and χ^2 test; $p < 0.05$ was considered significant.

Logistic Discriminant Analysis

To demonstrate the utility of differences in frequencies of cytologic parameters for LCNECs and SCLCs, a discriminant model was developed and evaluated. The frequencies of two cytologic features, in which differences were statistically significant, were regarded as two variables for a set of data, displayed as a scatter plot. By logistic discriminant analysis based on the scatter plots, a discriminant model for LCNEC and SCLC was made. When two variables for frequency of cytologic features were regarded as x_1 and x_2, the probability of an SCLC was calculated as follows.

$$P(SCLC) = \frac{\exp(-319.81 - 10.82x_1 + 16.30x_2)}{1 + \exp(-319.81 - 10.82x_1 + 16.30x_2)}$$

And the discriminant line was as follows.

$$-319.81 - 10.82x_1 + 16.30x_2 = 0 \Leftrightarrow x_2 = 19.62 + 0.6641x_1$$

We regarded a point on upper part of the line as true (SCLCs) and a point on lower part of the line as false (LCNECs). Furthermore, we analyzed prediction of error discrimination for new cases by leave-one-out cross validation. A discriminant model for LCNEC and SCLC was made except in one case. The excepted case was predicted by the discriminant model, and the discrimination confirmed whether it was correct. For all SCLC and LCNEC cases, the same analyses were performed repeatedly.

RESULTS

Clinical Findings

Clinicopathologic findings for the 29 LCNEC patients are summarized in Table 1. There were 26 men and 3 women, ranging in age from 48 to 80 years, with a median of 67 years. Lobectomy was performed on all. Mean follow-up time was 2.4 years (range, 0.33–9 years); 14 were dead, and 15 were alive at the time of this analysis. All patients had a smoking habit, ranging from 3 to 206.5 pack years. Of the 26 SCLC patients, 19 were men and 7 women, ranging in age from 58 to 80 years, with a median of 69 years. Eight were treated with surgical resection and eight with surgical resection after chemotherapy. In these 16 cases, no combination of SCLC with other histologic types was identified on resected materials. The remaining 10 underwent chemotherapy and/or radiotherapy, but again no admixture of other types was noted in biopsy specimens. Mean follow-up for the 26 patients was 2.6 years (range, 0.08–8 years); 14 were dead, and 12 were alive at the time of this analysis. All patients also had a smoking habit. A comparison of data for LCNEC and SCLC groups revealed no statistically significant differences in age, gender, and smoking status (Table 1).

Cytologic Findings

The initial cytologic diagnoses of 29 LCNEC patients were 4 LCNECs, 5 SCLCs, 2 combined SCLCs and adenocarcinomas, 5 neuroendocrine carcinomas, 1 atypical carcinoid, 7 poorly differentiated adenocarcinomas, 3 poorly differentiated squamous cell carcinomas, and 2 nonsmall cell carcinomas. In the LCNEC group, the unanimity in diagnosis between pathology and cytology was 21.1%. The cytologic

TABLE 1. Clinicopathologic Findings for LCNEC and SCLC Cases

Characteristic	No. of Patients	LCNEC (n = 29)	SCLC (n = 26)	p
Age (yr)				
<65	14	9	5	0.32
≤65	41	20	21	
Gender				
Male	45	26	19	0.11
Female	10	3	7	
Smoking status				
Nonsmoker	0	0	0	1.00
Smoker	55	29	26	
Cytologic materials				
TBAC	34	16	18	0.56
IC	5	3	2	
TBAC and IC	16	10	6	
Cytologic diagnosis				
LCNEC	4	4	0	<0.0001
LCNEC > SCLC	2	2	0	
NE	4	4	0	
SCLC	31	5	26	
SCLC + NSCLC	2	2	0	
NSCLC	12	12	0	
Tumor location				
Right lung	5	—	5	—
RUL	15	12	3	
RLL	12	7	5	
Left lung	2	—	2	
LUL	14	9	5	
LLL	7	1	6	
Type of location				
Central	11	3	8	0.09
Peripheral	44	26	18	
Tumor size (cm)				
≤3.0	25	12	13	—
>3.0	24	17	7	
NA	6	0	6	
Pathologic stage (pTNM)				
IA	14	8	6	—
IB	12	11	1	
IIA	5	1	4	
IIB	4	3	1	
IIIA	8	4	4	
IIIB	2	1	1	
IV	6	1	5	
NA(LD)	4	—	4	
Survival after surgery				
Dead	28	14	14	0.68
Alive	27	15	12	
Mean ± SD		2.39 ± 2.27	2.63 ± 2.33	

TBAC, transbronchial aspiration cytology; IC, imprint cytology; LCNEC, large cell neuroendocrine carcinoma; SCLC, small cell lung carcinoma; NE, neuroendocrine carcinoma; NSLC, nonsmall cell lung carcinoma; RUL, right upper lobe; RLL, right lower lobe; LUL, left upper lobe; LLL, left lower lobe; NA, not available; pTNM, from Ref. 15; LD, Limited disease.

TABLE 2 Cytologic Comparison Between LCNEC and SCLC

Cytologic Parameters	LCNEC (n = 29)	SCLC (n = 26)	p value
Necrotic background	25/29 (86.2%)	23/26 (88.5%)	0.802
Predominant cellular arrangement			
Cluster	26/29 (89.7%)	5/26 (19.2%)	
Single cells	3/29 (10.3%)	21/26 (80.7%)	<0.0001
Presence of characteristic clusters			
Large sized	27/29 (93.1%)	4/26 (15.4%)	<0.0001
Strong cohesion	27/29 (93.1%)	3/26 (11.5%)	<0.0001
Presence of tumor cell arrangement			
Rosette	28/29 (96.6%)	21/26 (80.7%)	0.061
Molding	26/29 (89.7%)	26/26 (100 %)	0.092
Pair cells	12/29 (41.3%)	17/26 (65.4%)	0.075
Palisading	27/29 (93.1%)	3/26 (11.5%)	<0.0001
Mean tumor cell size	178.1 μm^2	127.2 μm^2	<0.0001
Presence of characteristic tumor cells			
Large sized	18/29 (62.0%)	20/26 (76.9%)	0.224
Evidently identifiable cytoplasm	27/29 (93.1%)	20/26 (76.9%)	0.089
Prominent nucleoli	24/29 (82.8%)	20/26 (76.9%)	0.589
Small sized without prominent nucleoli	15/29 (51.7%)	26/26 (100 %)	<0.0001
Chromation pattern			
Finely granular	10/29 (34.5%)	11/26 (42.3%)	
Finely granular to granular	14/29 (48.3%)	15/26 (57.7%)	0.085
Granular	5/29 (17.2%)	0/26 (0 %)	
Presence of characteristics			
Mitoses	25/29 (86.2%)	25/26 (96.2%)	0.200
Nuclear streaking	26/29 (89.7%)	25/26 (96.2%)	0.354
Naked nuclei	24/29 (82.8%)	10/26 (38.5%)	0.0007

diagnoses for the 26 SCLC patients were all SCLCs, with statistically significant unanimity ($p < 0.0001$).

In a preliminary study, we evaluated any cytologic differences between aspiration smears and touch preparations in pilot groups consisting of 10 cases each of LCNEC and SCLC. In these groups, aspiration preparations and imprints showed no significant differences in any of the parameters chosen for assessment (data not shown). Comparisons between LCNEC and SCLC for each cytologic parameter are shown in Table 2. Cytologic parameters with statistically significant differences were as follows: cellular arrangement, presence of large clusters, tumor cell cohesion, palisading arrangement of tumor cells, mean of cellular areas, and presence of small cells without prominent nucleoli and naked nuclei. With regard to cellular arrangement, single cells were evident in all SCLC cases, whereas tumor cell clusters were frequently observed in LCNECs (Figures 1, 2). In the LCNEC group, although single cells were evident, many of them had naked nuclei. In particular, large clusters consisting of more than 60 cells were characteristic in LCNEC group

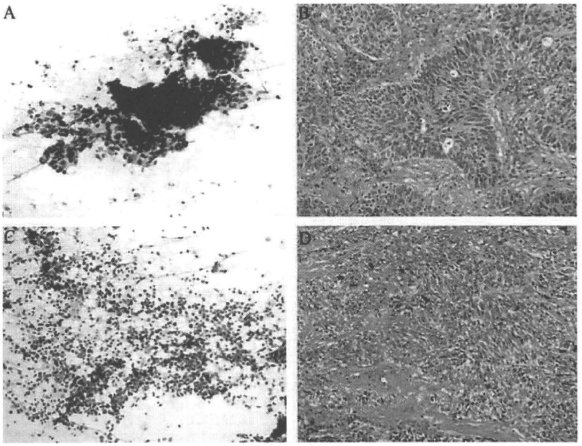

FIGURE 1. Photomicrographs illustrating cellular arrangement in transbronchial aspiration or histology specimens of LCNEC and SCLC cases. *A*, Large and three-dimensional clusters are conspicuous in a cytologic smear of an LCNEC case (Papanicolaou stain, ×20); *B*, tumor nests of an LCNEC case show palisading and Rosette-like formations in a histology specimen (hematoxylin and eosin stain, ×40); *C*, single cells are conspicuous in the cytologic smear of an SCLC case (Papanicolaou stain, ×20); and *D*, tumor cells of an SCLC case comprise irregular nests in a histology specimen (hematoxylin and eosin stain, ×40).

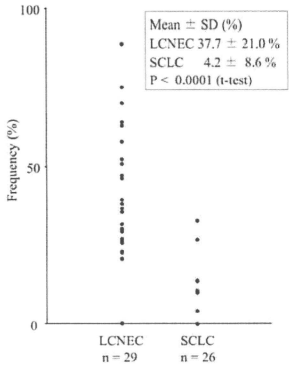

FIGURE 2. Frequencies of large clusters with tight cohesion in the LCNEC and SCLC groups (n = 55).

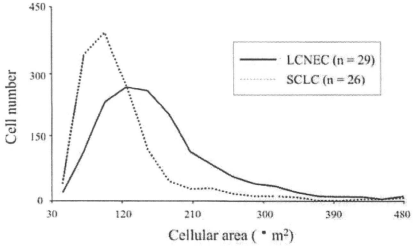

FIGURE 3. Histograms of cell areas in LCNEC and SCLC groups. Note that about 60% of the SCLC cells fall in the range of less than 120 μm^2, as compared with about 25% for LCNEC cells ($p < 0.0001$).

(Figures 1, 2). Also, on those histologic specimens, cell adhesion between tumor cells of LCNEC cases was conspicuous, whereas it was indistinct in SCLC cases (Figures 1*B*, *D*).

Furthermore, tumor cell cohesion was weak in SCLC cases, whereas in LCNEC cases tightly cohesive clusters predominated (Table 2). Frequencies of large clusters with tight cohesion are shown in Figure 3. The mean frequency was 37.7 ± 21.0% in the LCNEC cases and 4.2 ± 8.4% in SCLCs, the difference being statistically significant ($p < 0.0001$). LCNEC cases featured discrete cell nests divided by fibrous stroma with frequent peripheral palisading, whereas SCLC cases were characterized by cell nests, frequently infiltrating adjacent fibrous stroma (Figure 1).

Mean cell areas were 178.1 ± 84.8 μm^2 (range, 45.3–808.9 μm^2) for LCNEC cases and 127.8 ± 69.3 μm^2 (range, 36.8–699.5 μm^2) for SCLCs, the difference being statistically significant ($p < 0.0001$). The distributions are shown graphically in Figure 3. Some 58.2% of the SCLC cells (756/1300) were less than 120 μm^2, as compared with only 24.6% for LCNEC cells (357/1450; $p < 0.0001$). Furthermore, small tumor cells lacking prominent nucleoli in SCLC cases were observed more frequently than in LCNEC cases ($p < 0.0001$; Table 2 and Figure 5). Frequencies are shown in Figure 4. The mean values were 11.9 ± 12.1% in LCNEC and 55.8 ± 18.9% in SCLC cases, the difference being

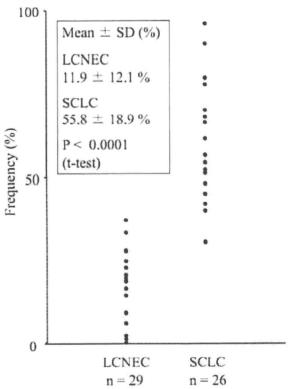

FIGURE 4. Frequencies of small tumor cells without prominent nucleoli in the LCNEC and SCLC groups (n = 55).

statistically significant ($p < 0.0001$). Also, in histologic specimens, SCLC cases had the cell nests predominantly composed of small tumor cells with scant cytoplasm without nucleoli, whereas LCNEC cases demonstrated cell nests predominantly composed of large tumor cells with abundant cytoplasm and occasional prominent nucleoli (Figure 5*B*, *D*).

Logistic Discriminant Analysis

For the frequencies of large clusters with tight cohesion and small tumor cells without prominent nucleoli, statistically significant differences with strong power was evident between LCNEC and SCLC groups. Therefore, these two cytologic parameters were considered as the two variables for the scatter plots. The dots for LCNEC cases are located on the lower right, whereas those of SCLC cases were located on the upper left, with clear differences between the two for the majority. The results of logistic discriminant analysis are shown in Figure 6. Because all SCLC and LCNEC cases were cytologically discriminated accurately, sensitivity, specificity, and accuracy were all 100%. Moreover, the results of leave-one-out cross validation, shown in Figure 7, gave a predicted error rate of (2 + 1)/55 = 0.00545.

DISCUSSION

In this study, the large cell cluster with tight cohesion was confirmed to be a valuable cytologic feature, allowing distinction between LCNECs and SCLCs. Although other reports on cytologic features of LCNECs described that cell cohesion of LCNECs was reduced as in SCLC,[17–22] the difference was highly significant in our series. However, palisade arrangement was described as a one point for cytologic distinction of LCNEC from SCLC,[17–22] and it was considered to be easy to detect tight cell cohesion by light microscope. Therefore, it should be emphasized that focusing on large clusters with tight cohesion is most important for cytologic discrimination between LCNECs and SCLCs.

Several authors showed that tumor cells of LCNECs had similar morphologic features to SCLCs except for cell size, this being significantly larger for LCNECs than SCLCs.[17–22] In these series, a majority of the SCLC cells were less than 120 μm^2 in size, statistically significant as compared with LCNEC cells ($p < 0.0001$). Another characteristic was that most of small cells in SCLC cases had no

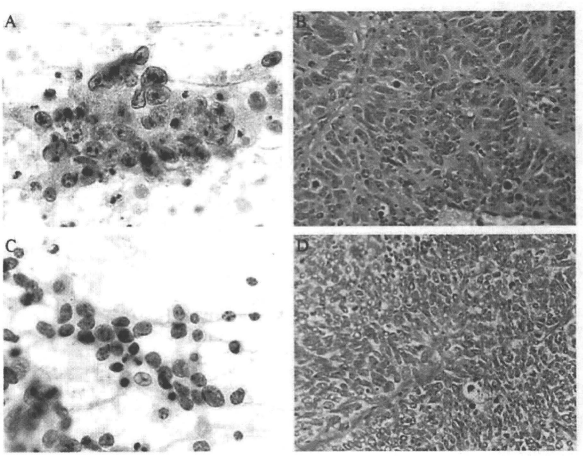

FIGURE 5. Photomicrographs illustrating single cells and tissue architecture in LCNEC and SCLC cases. *A*) Tumor cells ≥120 μm^2 and/or with prominent nucleoli are evident in a cytologic smear of an LCNEC case (Papanicolaou stain, ×100); *B*, nests of LCNEC cells are predominantly composed of large tumor cells with abundant cytoplasm and occasional prominent nucleoli (hematoxylin and eosin stain, ×40); *C*, tumor cells <120 μm^2 without prominent nucleoli are evident in a cytologic smear of an SCLC case (Papanicolaou stain, ×100); *D*, nests of SCLC cells are predominantly composed of small tumor cells with scant cytoplasm without nucleoli (hematoxylin and eosin stain, ×40).

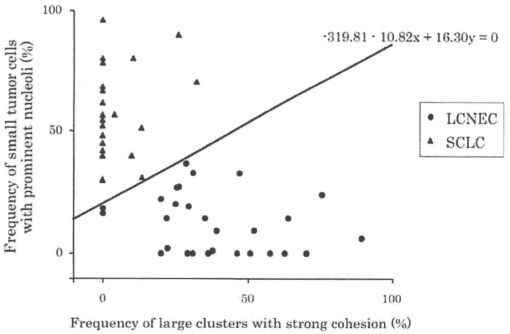

FIGURE 6. Logistic regression for frequencies of small tumor cells without prominent nucleoli and large clusters with tight cohesion. The scatter plot allows clear separation of LCNEC (●) and SCLC cases (▲) by the calculated discriminant line. Therefore, a discriminant model for LCNEC and SCLC, diagnosing as SCLCs if dots exist in the field above the line and as LCNECs if below the line, was made. All SCLC and LCNEC cases were discriminated correctly with the discriminant model based on logistic regression from cytologic frequencies, and sensitivity, specificity, and accuracy were all 100%.

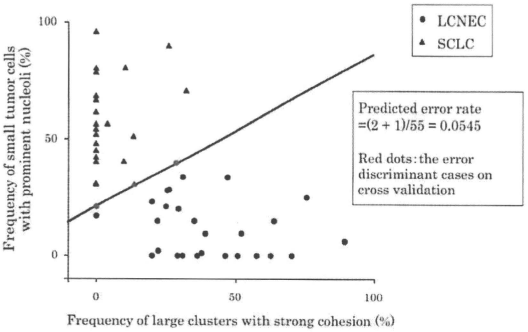

FIGURE 7. Leave-one-out cross validation. Regarding each case as a new case, prediction of the error rate of the discriminant model was analyzed. Red dots show error discriminant cases on cross validation. Two of the LCNEC cases and one SCLC case were discriminated in error with the discriminant model, so that the prediction of error rate of the model was 0.00545.

prominent nucleoli, again being significantly different from LCNECs ($p < 0.0001$). Moreover, although naked nuclei appear to be a significant distinguishing attribute between the two tumor types, it was considered to be inadequate for inclusion in the discriminant model for the following reasons: it is rather difficult to perceive cytoplasm in intact large cells compared with small cells, and naked nuclei was not found in more than 60% of SCLC cases. Therefore, only the frequency of the small cells without prominent nucleoli contributed to cytologic discrimination between LCNEC and SCLC.

To establish accurate cytologic diagnosis of LCNEC using the two cytologic parameters, we established a discriminant model that gave exceedingly good sensitivity, specificity, and accuracy. The current discriminant model, however, does have some problems with routine cytology as follows: complicated procedures for obtaining the two cytologic parameters and necessity of uniform diagnostic criteria among cytopathologists. However, with greater experience of LCNEC cases and grasp of detailed cytologic features, it should be possible to overcome these problems.

In conclusion, our discriminant model based on the cytologic features of large cell clusters with tight cohesion and of small tumor cells without prominent nucleoli should prove a useful aid for distinction between LCNECs and SCLCs particularly. Prospective large-sized studies including other nonsmall cell lung cancers are now required to assess the diagnostic impact of this model with routine cytology.

ACKNOWLEDGMENTS

Supported by a Grant-in-aid from the Ministry of Education, Sports, Culture, Science and Technology grant 20591676, Ministry of Health, Labor and Welfare grant 19-12, and the Vehicle Racing Commemorative Foundation grant.

The authors thank Drs. Masaru Ushijima and Masaaki Matsuura, Bioinformatics Group, Genome Center, Japanese

Foundation for Cancer Research, for helpful advice with the statistical analyses.

REFERENCES

1. Cooper WA, Thourani VH, Gal AA, et al. The surgical spectrum of pulmonary neurocrine neoplasms. *Chest* 2001;119:14–18.
2. Garcia-Yuste M, Matilla JM, Alvarez-Gago T, et al. Prognostic factors in neuroendocrine lung tumors: a Spanish multicenter study. *Ann Thorac Surg* 2000;70:258–263.
3. Jones MH, Virtanen C, Honjoh D, et al. Two prognostically significant subtypes of high-grade lung neuroendocrine tumors independent of small-cell and large-cell neuroendocrine carcinomas identified by gene expression profiles. *Lancet* 2004;363:775–781.
4. Travis WD, Linnoila RI, Tsokos MG, et al. Neuroendocrine tumors of the lung with proposed criteria for large cell neuroendocrine carcinoma. An ultrastructural, immunohistochemical, and flow cytometric study of 35 cases. *Am J Surg Pathol* 1991;15:529–533.
5. Asamura H, Kameya T, Matsuno Y, et al. Neuroendocrine neoplasms of the lung: a prognostic spectrum. *J Clin Oncol* 2006;24:70–76.
6. Dresler CM, Ritter JH, Patterson GA, et al. Clinical-pathologic analysis of 40 patients with large cell neuroendocrine carcinoma of the lung. *Ann Thorac Surg* 1997;63:180–185.
7. Fernandez FG, Battafarano RJ. Large cell neuroendocrine carcinoma of the lung. *Cancer Control* 2006;13:270–275.
8. Hiroshima K, Iyoda A, Shida T, et al. Distinction of pulmonary large cell neuroendocrine carcinoma from small cell lung carcinoma: a morphological, immunohistochemical, and molecular analysis. *Mod Pathol* 2006;19:1358–1368.
9. Iyoda A, Hiroshima K, Nakatani Y, et al. Pulmonary large cell neuroendocrine carcinoma: its place in the spectrum of pulmonary carcinoma. *Ann Thorac Surg* 2007;84:702–707.
10. Iyoda A, Hiroshima K, Toyozaki T, et al. Adjuvant chemotherapy for large cell carcinoma with neuroendocrine features. *Cancer* 2001;92: 1108–1112.
11. Jiang SX, Kameya T, Shoji M, et al. Large cell neuroendocrine carcinoma of the lung: a histologic and immunohistochemical study of 22 cases. *Am J Surg Pathol* 1998;22:526–537.
12. Travis WD, Gal AA, Colby TV, et al. Reproducibility of neuroendocrine lung tumor classification. *Hum Pathol* 1998;29:272–279.
13. Wick MR, Berg LC, Herts MI. Large cell carcinoma of the lung with neuroendocrine differentiation: a comparison with large cell "undifferentiated" pulmonary tumors. *Am J Surg Pathol* 1992;97:796–805.
14. Veronesi G, Morandi U, Alloisio M, et al. Large cell neuroendocrine carcinoma of the lung: a retrospective analysis of 144 surgical cases. *Lung Cancer* 2006;53:111–115.
15. Travis WD, Colby TV, Corrin B, et al. *Histological Typing of Lung and Pleural Tumors*. 3rd Ed. *World Health Organization International Histological Classification of Tumors*. Berlin: Springer Verlag, 1999.
16. Colby TV, Koss MN, Travis WD. *Tumors of the Lower Respiratory Tract. Atlas of Tumor Pathology*. 3rd series. Washington DC: Armed Forces Institute of Pathology, 1995:248–255.
17. Hiroshima K, Abe S, Ebihara Y, et al. Cytological characteristics of pulmonary large cell neuroendocrine carcinoma. *Lung Cancer* 2005;48: 331–337.
18. Iyoda A, Baba M, Hiroshima K, et al. Imprint cytologic features of pulmonary large cell neuroendocrine carcinoma: comparison with classic large cell carcinoma. *Oncol Rep* 2004;11:285–288.
19. Jimenez-Heffernan JA, Lopez-Ferrer P, Vicandi B, et al. Fine-needle aspiration cytology of large cell neuroendocrine carcinoma of the lung: a cytopathologic correlation study of 11 cases. *Cancer* 2008;114:180–186.
20. Kakinuma H, Mikami T, Iwabuchi K, et al. Diagnostic findings of bronchial brush cytology for pulmonary large cell neuroendocrine carcinomas. *Cancer (Cancer Cytopathol)* 2003;99:247–254.
21. Nicholson SA, Ryan MR. A review of cytologic findings in neuroendocrine carcinomas including carcinoid tumor with histologic correlation. *Cancer (Cancer Cytopathol)* 2000;90:148–161.
22. Wiatrowska BA, Krol J, Zakowski MF. Large cell neuroendocrine carcinoma of the lung: proposed criteria for cytologic diagnosis. *Diagn Cytopathol* 2001;24:58–64.
23. Nicholson SA, Beasley MB, Brambilla E, et al. Small cell lung carcinoma (SCLC): a clinicopathologic study of 100 cases with surgical specimens. *Am J Surg Pathol* 2002;26:1184–1197.

Clin Exp Metastasis (2010) 27:389–397
DOI 10.1007/s10585-010-9313-4

RESEARCH PAPER

Lung cancer progression and metastasis from the prognostic point of view

Kentaro Inamura · Yuichi Ishikawa

Received: 7 March 2009 / Accepted: 16 February 2010 / Published online: 12 March 2010

Abstract Lung cancer is the leading cause of cancer death in men and women worldwide. Since the occurrence of metastases in distant organs is the major reason for mortality of cancer patients, we need to elucidate the underlying mechanisms. Many studies featuring analysis of gene expression, comparative genomic hybridization and loss of heterozygosity analysis have been performed and generated support for the hypothesis that metastatic potential is acquired early in tumorigenesis. Furthermore, it is now clear that the majority of tumor cells have the potential to metastasize. Although many changes in gene expression profiles have been established retrospectively, translational research is now a high priority to enable clinical application and treatment based on laboratory findings.

Keywords Lung cancer · Metastasis · Prognosis · Gene expression · Comparative genomic hybridization · Loss of heterozygosity analysis

Introduction

Lung cancer, the leading cause of cancer death in men and women worldwide and continuing to rise in frequency, is generally classified as of either small-cell lung carcinoma (SCLC) or non-SCLC (NSCLC) types. Within these groups further distinctions are made, with NSCLCs sub-divided into adenocarcinomas, squamous cell carcinomas (SCCs), and large cell carcinomas (LCCs). The occurrence of metastases in distant organs is the major cause of death for the vast majority of lung cancer patients. Clinical outcomes can be roughly predicted by pathological-Stage (p-Stage) and 5 year survival for p-Stage I cases, pathologically lacking metastases, is relatively good, ranging from 60 [1] to 90% [2]. Even when cancer lesions have been fully removed and no metastasis is found at surgery, however, some patients with p-Stage I lesions suffer recurrence and die of cancer relapse. Presumably, these already had micrometastases at the time of tumor removal. To avoid unnecessary lymph node dissection in low-risk cases but ensure that postoperative adjuvant therapy is performed for high-risk patients, we need a clinically useful approach to better stratify patients with respect to the risk of recurrence. Towards a rational treatment, we need to elucidate metastatic gene signatures and molecular mechanisms of lung cancer progression. The aim of the present review is to survey findings on lung cancer progression and metastasis from the prognostic point of view, especially emphasizing our study [3] paying attention to heterogeneity of lung cancers, an important characteristic.

K. Inamura · Y. Ishikawa (✉)
Department of Pathology, The Cancer Institute, Japanese Foundation for Cancer Research (JFCR), 3-10-6 Ariake, 135-8550 Koto-ku, Tokyo, Japan
e-mail: ishikawa@jfcr.or.jp

The beginning of gene expression profiling in lung cancers

In November, 2001, pioneering studies of gene expression profiling in lung cancers were reported at the same time by a Stanford University group [4] and a Harvard University group [5]. Subdivision of the tumors based on gene expression faithfully recapitulated their histological classification and characteristic expression profiles for each histological type could be identified. The insulinoma-associated gene 1 (IA-1) and the human achaetescute homolog 1 (hASH1) were found to be neuroendocrine SCLC markers, shared also

by carcinoid tumors. Identified as SCC markers were Keratin 5 (KRT5), KRT17 and Tumor protein p63, which is associated with development of squamous epithelium. Supporting the traditional view that lung adenocarcinomas are a heterogeneous group, distinct subclasses were evident. One adenocarcinoma subgroup was comprised of tumors expressing neuroendocrine markers, such as hASH1 and IA-1, associated with a significant decrease in patient survival when compared to other adenocarcinomas [5]. Another subgroup appeared to express markers of alveolar type II pneumocytes and was characterized by high relative expression of TTF1 or surfactant protein genes.

Gene expression profiling predicting survival of patients with lung adenocarcinomas

As mentioned above, the Stanford University group [4] and the Harvard University group [5] first identified prognostically different subgroups of adenocarcinomas by gene expression profiling. One subgroup with a poor prognosis was revealed to have neuroendocrine features. Subsequently, many further studies using gene expression profiling have been reported. Beer et al. [6] described development of a risk index, compiling the relative expression of 50 genes, to identify high or low risk groups of Stage I adenocarcinomas that correlated with patient survival.

Ramaswamy et al. [7] compared gene expression profiles of adenocarcinoma metastases and unmatched primary adenocarcinomas and found patterns that allowed distinction between the two, but also reported that a subset of primary tumors had similar expression to metastases. This finding led them to challenge "the notion that metastases arise from rare cells within the primary tumor." They suggested that the majority of tumor cells have the potential to metastasize, but this remains controversial and Liotta and Kohn have argued against their conclusions [8]. When lists of genes are examined, it is unclear whether the expression profile is a cause or a local consequence of the metastatic process. Ramaswamy et al. did not microdissect tumor cells for analysis of their tissue specimens and consequently the gene-expression pattern data reflect contributions from multiple cell populations. Thus, the expression pattern of the genes in the authors' signature set may be at least partially due to activated host stromal elements. Indeed, two of the important upregulated genes in the list encode stromal collagen.

Although gene expression profiles that can classify cancer patients according to the risk of recurrence have been found, most studies have been retrospective. Very recently, Potti et al. [9] documented a "lung metagene model" that can identify individuals at increased risk for disease recurrence with stage IA NSCLC, which they now plan to use for a prospective randomized clinical trial. Translational research is now an urgent priority to enable clinical application of basic research findings.

Gene expression profiling using hierarchical clustering and non-negative matrix factorization in squamous cell carcinomas

After the adenocarcinoma, the SCC is the most frequent lung cancer histology, accounting for approximately 30% of the total. Its development is the most strongly related to smoking. For adenocarcinomas, subclassification by differentiation grade [10] or histological pattern [2] is useful to predict prognosis. For SCCs, differentiation grade is used for pathological subclassification, but it correlates poorly with prognosis. Although SCCs demonstrate some histological variation, such as with the basaloid variant, this does not allow good prediction of prognosis. The present system used to subclassify SCC is thus insufficient and we have therefore attempted to make a clinically useful classification based on gene expression profiling [11]. By hierarchial clustering, we subclassified SCCs into two prognostically significant subclasses. Furthermore, consensus clustering with a non-negative matrix factorization (NMF) approach indicated the robustness of this classification (Fig. 1). NMF appears to be more accurate for choice of input genes than hierarchial clustering and can be combined with a quantitative evaluation of the robustness with numbers of clusters [12]. Both hierarchical clustering and NMF approaches (Fig. 1) indicated that SCCs can be divided into two groups, SCC-A and SCC-B, with prognostic variation (Fig. 2a). The cophenetic correlation coefficient, k, quantitatively indicated the two-centroid clustering to be the most robust with the highest value, as attested by clear block diagonal patterns (Fig. 2b). Up-regulation of cell-proliferation-related genes was evident in the subclass with poor survival. In the subclass with better survival, genes involved in differentiated intracellular functions, such as the MAPKKK cascade, ceramide metabolism, or regulation of transcription, were upregulated.

Histological typing and gene expression profiles in high-grade neuroendocrine tumors

The current WHO classification of high-grade neuroendocrine tumors (HGNTs) currently recognizes large-cell neuroendocrine carcinoma (LCNEC), a subclass of LCC, and SCLC as a distinct group [13]. Since LCNEC and SCLC share several histological features, a consensus differential diagnosis between LCNEC and SCLC is sometimes difficult, even among experienced lung pathologists. Hence, by the microarray technique, we analyzed gene

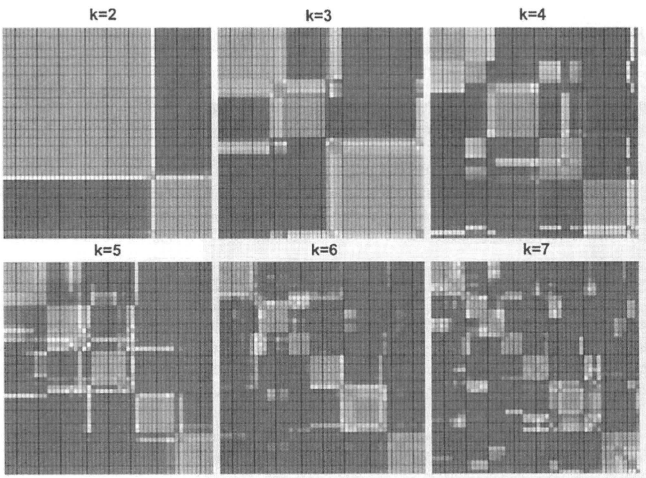

Fig. 1 Reordered consensus averaging 50 connectivity matrices computed at $k = 2$–7 for all SCC samples with 3,344 genes. Samples were hierarchically clustered, colored from 0 (samples never in the same cluster) to 1 (samples always in the same cluster)

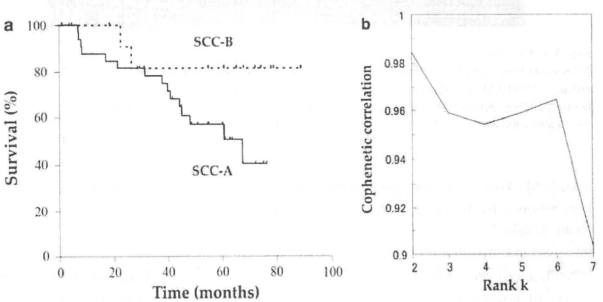

Fig. 2 **a** Kaplan–Meier survival curves for the 48 SCC patients (SCC-A vs. SCC-B). **b** Cophenetic correlation coefficients for the hierarchically clustered matrices

expression profiles of HGNTs with other histological tumor groups and normal lung tissue [14]. By hierarchical clustering, we could readily identify distinct groups for carcinoids, LCC, adenocarcinoma, and normal lung (Fig. 3a). While we could not subclassify SCLC and LCNEC by gene expression profiling, two prognostically significant subtypes of HGNT were evident, independent of SCLC and LCNEC ($P = 0.0094$). Many genes distinguished the HGNT groups. There was no significant difference in survival between SCLC and LCNEC samples (Fig. 3b; $P = 0.37$).

Integrated classification of lung tumors and cell lines by expression profiling

The utility of cancer cell lines depends largely on their accurate classification, commonly based on histopathological diagnosis of the cancers from whom they were derived. However, because cancers are often heterogeneous, cell lines, which also have a propensity to alter in vitro, may not be truly representative. We therefore performed gene expression profiling, which can faithfully recapitulate histological classification of tumors, to examine different cell

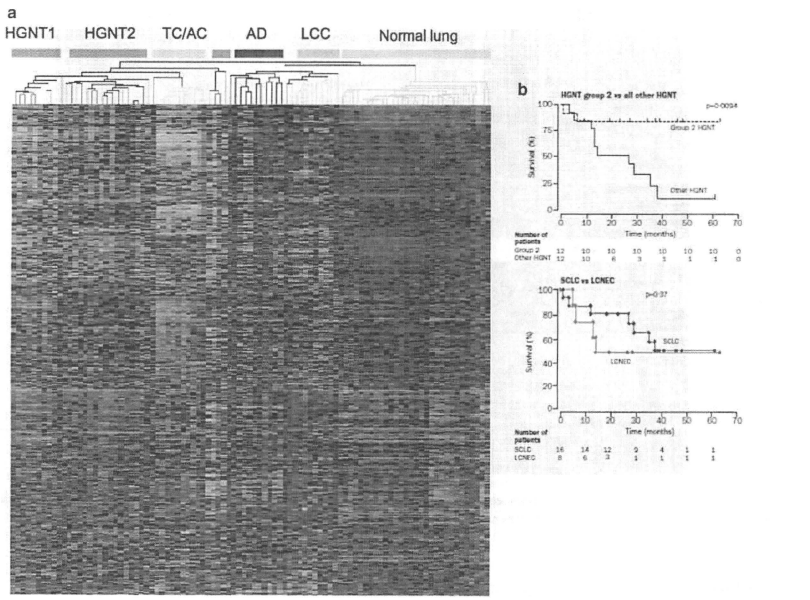

Fig. 3 **a** Unsupervised hierarchical clustering of 64 lung cancer and 30 normal lung samples against 2,803 genes with expression differentially regulated in neuroendocrine tumors. *HGNT* high grade neuroendocrine tumor, *TC/AC* typical carcinoids/atypical carcinoids, *AD* adenocarcinoma, *LCC* large cell carcinoma. **b** Kaplan-Meyer survival curves for patients with HGNTs in group 2 and all other HGNTs and for histopathologically diagnosed SCLC versus LCNEC. SCLC, small-cell lung carcinoma; LCNEC, large-cell neuroendocrine carcinoma

lines [15]. After excluding genes which show clear distinction between fresh and cell-line samples, hierarchical clustering resulted in a large degree of integration of cell lines into four main tumor branches, an SCLC branch, a SCC branch, a cell-line branch, and a branch containing normal tissue, adenocarcinoma and LCC (Fig. 4). As a result, most of SCC cell lines or SCLC cell lines grouped with fresh SCC tumors or fresh SCLC tumors, respectively. In contrast, although none of adenocarcinoma cell lines clustered with fresh adenocarcinoma tumors, some of them clustered with fresh SCC tumors or fresh SCLC tumors. Adenocarcinomas may ultimately progress toward one of two poorly differentiated phenotypes with expression profiles resembling SCC or SCLC. Our observations suggest that adenocarcinoma cell lines either dedifferentiate toward molecular pathologies resembling SCLC or SCC, or that clonal expansion of SCC or SCLC subcomponents occurs frequently. Analysis of larger numbers of adenocarcinoma samples taken at the time of surgery and autopsy will be required to verify that adenocarcinomas develop similarly in situ.

Comparison of accumulated allele loss between primary lung tumors and lymph node metastases

Sasatomi et al. [16] have compared loss of heterozygosity (LOH) at microsatellites between primary NSCLCs and their lymph node metastases, calculating fractional allele loss (FAL), defined as the ratio of chromosomes affected by LOH in the informative chromosomes, for each sample. With Stage II NSCLCs, the FAL was found to be significantly less in the metastatic sites compared with the primary neoplasms. The authors advanced the theory that this phenomenon was the result of early metastatic spread of the carcinoma, with the primary neoplasm then acquiring additional genetic changes. This concept should be borne in mind when comparing molecular profiles of

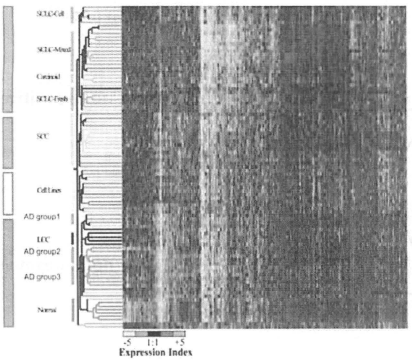

Fig. 4 Dendrogram of the reduced data set of 4,253 genes after filtering for commonly regulated genes in either fresh or cell-line samples. Groupings indicated on the *left* represent distinct clusters of particular carcinoma types. AD, adenocarcinoma; Normal, normal lung tissue

primary neoplasms with those of metastatic or recurrent sites.

Gene expression profile for tissue-specific metastasis

Kang et al. [17] have identified, in a human breast cancer cell line, a specific set of genes that mediates metastasis to bone. They suggested that primary tumors with metastatic capacity possess the poor-prognosis signature but, additional functions, provided by a set of bone metastasis genes, must be expressed in order to achieve an overt, tissue-specific metastasis phenotype. Organ-specific expression profiles for human small-cell lung cancer metastases in mice have also been reported by Kakiuchi et al. [18], but it remains unclear whether these might already be present in the parental cells.

Heterogeneity of primary tumors and metastatic potential

Introduction

Recent microarray experiments have suggested that the majority of cancer cells have the potential to metastasize, with obvious clinical and therapeutic implications, not only in breast cancers [19], but also in lung cancers [7]. Ramaswamy et al. [7] identified a molecular signature of metastatic potential within the bulk of each primary lung cancer, suggesting that metastatic potential is in fact acquired early and is a feature of the majority of lung cancer cells. To test this hypothesis, we adopted the lung adenocarcinoma, which characteristically shows widespread intratumoral heterogeneity, as a model [3].

The mixed type adenocarcinoma in the lung, which shows a variety of histological subtypes, is the most frequent subtype in the WHO classification criteria [13], accounting for approximately 80% of resected lung adenocarcinomas [20]. An invasive component with high cellular and structural atypia is often included but peripherally well-differentiated components with low atypia may also be present (Fig. 5). Is the metastatic signature detected only in the aggressive component with high atypia? Or is it present in the entire tumor irrespective of morphological heterogeneity? If the latter is true, then it follows that the metastatic potential is acquired early in tumor progression and the entire tumor, including the morphologically less malignant component, may have metastatic potential.

Using lymph node-positive lung adenocarcinomas, we compared gene expression profiles among moderately-differentiated components with aggressive appearance, peripheral well-differentiated components with less malignant appearance, and patient-matched lymph node metastases. Node-negative lung adenocarcinomas, which are morphologically indistinguishable from node-positive tumors, were included for comparison and differential diagnosis.

Schematic design

The schematic design for this study is shown in Fig. 5. We analyzed 10 pairs of primary lung adenocarcinomas and their synchronous lymph node metastases and 11 primary lung adenocarcinomas without lymph node or organ metastases. With the 21 primary lung adenocarcinomas, we isolated tumor cells from predominant moderately-differentiated components. In five of the 10 node-positive primary lung adenocarcinomas, we additionally isolated peripheral well-differentiated components. To focus selectively on cancer cells, we applied laser capture microdissection (LCM). For comparison, we included six samples of macrodissected normal lung tissue.

Experiments and results

Firstly, we wished to identify the overall gene expression signature in all 42 samples by unsupervised hierarchical clustering with a set of highly variable genes. Two-way hierarchical clustering was performed using a Pearson correlation (Fig. 6). Eight of the 10 pairs of primary and metastatic tumors clustered next to each other. In these cases, the metastatic tumors had a higher similarity to their matching primary tumors than to all other tumors. In only two of the node-positive cases (cases 5 and 9), the metastatic tumors did

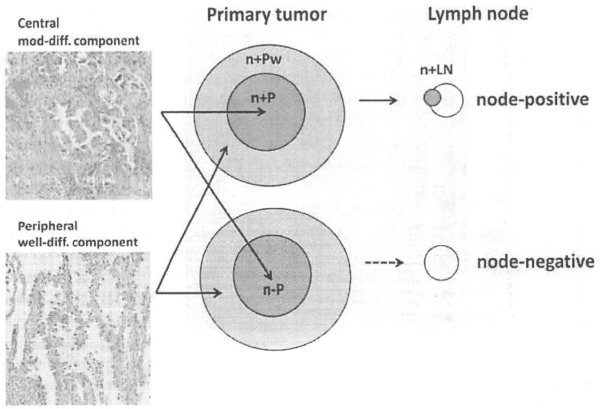

Fig. 5 Schematic design of this study. n + P, node-positive primary tumor; n-P, node-negative primary tumor; n + LN, node-positive lymph node; n + Pw, well-differentiated component of the node-positive primary tumor. Representative microscopic images of primary lung adenocarcinomas used in this study are shown, comprising moderately-differentiated components dominating large portions of the lesions and well-differentiated components evident in peripheral portions

not cluster with their matching primary tumors, but a substantial similarity was still observed. In addition, all the peripheral well-differentiated components showed tight clustering with the predominant moderately-differentiated components from the same primary tumors. In the overall gene expression signatures, the central and the peripheral components from the same primary tumor were strikingly similar to each other.

To identify the gene expression signature of lymph node metastases, we performed a statistical comparison between the 10 pairs of primary and metastatic tumors using a paired *t*-statistic. Only 12 genes were yielded. For 11 of these genes, no significant differences were found between 10 lymph node metastases and 11 node-negative primary tumors, suggesting that they are not part of a metastatic expression signature. Only one gene, *Chromosome 4 open reading frame 7* (*C4orf7*) was significantly higher in the lymph node metastases than both node-positive and -negative primary tumors. However, as *C4orf7* is expressed characteristically by follicular dendritic cells found in lymph nodes, the high expression presumably resulted from contamination in the LCM process. It follows that no significant metastatic changes were detected between primary tumors and their lymph node metastases. The marked similarity between primary tumors and their lymph node metastases drove us to consider that the gene expression signature of lymph node metastasis might be acquired by the majority of primary tumor cells.

Next, to identify the metastatic expression signature detected in the primary tumors, we performed a statistical comparison (Welch's *t*-test) between 10 node-positive primary tumors and 11 node-negative primary tumors. This yielded 75 genes, comprising 37 with significantly higher expression in node-positive than node-negative primary tumors and 38 with significantly lower expression. The top discriminating gene was *homeobox B2* (*HOXB2*) with

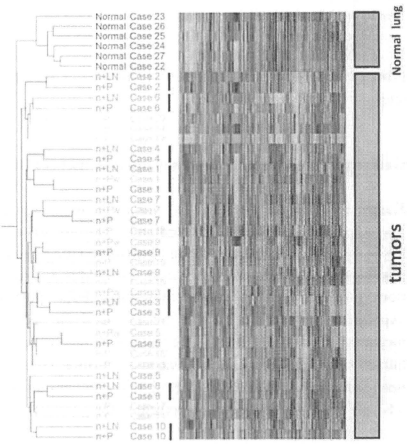

Fig. 6 Unsupervised hierarchical clustering for 2,451 genes against 42 samples comprising 10 pairs of node-positive primary tumors (n + P) and node-positive lymph nodes (n + LN), 11 node-negative primary tumors (n-P), 5 well-differentiated components of the node-positive primary tumors (n + Pw), and 6 normal tissues (Normal). Columns represent gene and rows represent samples. Note that eight of the 10 pairs of primary and metastatic tumors clustered next to each other (*bars*)

higher expression in node-positive primary tumors. Malignant potential associated with ectopic *HOXB2* expression has been reported recently [21]. Down-regulated genes in node-positive primary tumors include *VAMP-associated protein A* (VAPA), involved in vesicle trafficking, and *Zinc finger protein 36 homolog* (ZFP36), which is also known as *tristetraprolin* (TTP) and is involved in degradation of tumor necrosis factor α. The *IQ motif containing GTPase activating protein 1* (*IQGAP1*), one of the molecular markers for lymph node metastasis identified by a microarray study using LCM [22], was also found to be included in the down-regulated genes.

The next issue was whether this 75-gene signature might be maintained throughout the metastatic process, and also be present in peripheral well-differentiated components of primary tumors. We therefore performed supervised hierarchical clustering of all the 42 samples against these 75 genes using a Pearson correlation (Fig. 7). Node-positive cases formed a distinct independent group, except one case (case 9), separate from node-negative tumors and normal lung tissues. The latter two clustered together. The node-positive group included the metastatic tumors and the primary well-differentiated components. Also in this metastatic gene expression signature, as with the overall gene expression signature, samples from the same case showed tight clustering. In leave-one-out cross-validation analysis, the 75 genes predicted their groups with 100% accuracy. Using real-time RT-PCR analysis, we validated our results for some of genes of interest from the 75-gene set.

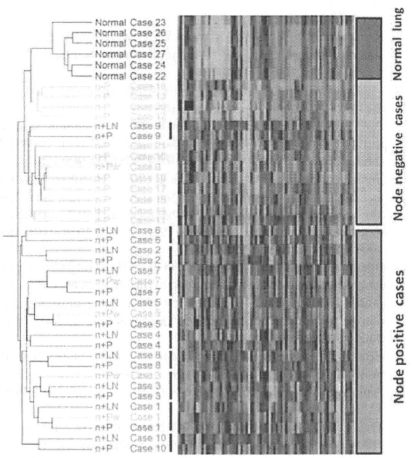

Fig. 7 Hierarchical clustering for the 75 genes against 42 samples comprising 10 pairs of node-positive primary tumors (n + P) and node-positive lymph nodes (n + LN), 11 node-negative primary tumors (n-P), 5 well-differentiated components of the node-positive primary tumors (n + Pw), and 6 normal tissues (Normal). Remarkably, nine of the 10 node-positive cases formed a distinct independent group. Pairs of primary and metastatic tumors clustered next to each other (*bars*)

Discussion

In this study, we could identify a 75-gene signature discriminating between node-positive and node-negative primary lung adenocarcinomas. Hierarchical clustering using this gene set generated a distinct independent group composed of node-positive cases, including the metastatic tumors and the peripheral well-differentiated components, separate from node-negative tumors and normal lung tissues. Striking transcriptional similarities were observed between samples from the same case and unsupervised hierarchical clustering showed tight clustering. Hierarchical clustering using the 75-gene set also showed tight clustering, reflecting similarity also in the metastatic gene expression signature. Indeed, statistical comparison of gene expression levels between pairs of primary tumors and their lymph node metastases revealed no differences responsible for the metastasis, implying that metastatic potential might be established early in the pathogenesis of tumors. This result is in keeping with recent array findings suggesting that metastatic potential is encoded in the bulk of a primary tumor [7]. More recently, D'Arrigo et al. [23] similalry showed striking transcriptional similarity using 10 pairs of matching primary colorectal cancers and distant metastases.

Several studies have resulted in lists of metastasis-related or malignancy-related genes in lung cancers [5–7, 22, 24]. However, most authors did not use microdissection but rather RNAs isolated from tumor masses. As their gene lists differed widely and had only few genes in common, the 75-gene list we identified also differed widely from theirs. Ein-Dor et al. [25] reported that thousands of samples are needed to generate a robust gene list for predicting outcome in cancer. Kikuchi et al. [22] used microdissected samples of 22 primary lung adenocarcinoma cases and identified 40 genes whose expression levels could separate cases according to their lymph node status. One of the 40 genes was *IQGAP1*, also included in our 75-gene metastatic signature. In our hospital, survival for p-Stage I lung cancer patients is good as compared with the literature. Whereas the reported 5-year survival for p-Stage I patients with non-small cell lung cancer is about 60% [1], it is 90% in our hospital [2]. We usually perform thorough dissection of lymph nodes and make a detailed histopathological examination. This accurate assessment of lymph node status is clearly advantageous for comparison of node-positive and node-negative tumors.

In the 75-gene set we identified, *HOXB2* was the top discriminating gene between node-positive and node–negative primary lung adenocarcinomas. Aberrant expression of *HOX* genes has been implicated in leukemias and various solid cancers, including lung cancers, with likely involvement of the gene products in features of malignant progression, such as invasion and metastasis. Overexpression of *HOXD3* is known to induce coordinate expression of metastasis-related genes in lung cancer cells [26]. A recent study further revealed ectopic *HOXB2* expression in pancreatic cancers and some proportion of precursor lesions, pancreatic intraepithelial neoplasias, possibly associated with a poor prognosis [21]. In our current study, we observed *HOXB2* overexpression not only in the central but also in the peripheral zones of node-positive primary tumors. Malignant potential associated with *HOXB2* expression might thus be acquired early in tumorigenesis.

Our results imply that the metastatic potential might be encoded in the entirety of each primary lung tumor including the morphologically less malignant component. This has profound clinical implications. It offers a rationale for therapeutic applications based on the expression profile of the primary tumor. Even if the peripheral component of the tumor is sampled by bronchoscopic or needle biopsy, the metastatic potential of the tumor could be predicted with accuracy. Such evaluation of metastatic potential would help spare unnecessary lymph node dissection for low-risk patients. However, the 75-gene signature needs to be confirmed using independent samples and further research is required to clarify the included molecular functions.

Very recently, using real time RT-PCR analysis, we investigated the transcriptional levels of the top metastasis-related genes using 96 independent test lung adenocarcinoma samples and investigated their correlations with prognosis [27]. We could document evidence that p-Stage I patients with HOXB2 up-regulation have a worse prognosis than those with HOXB2 down-regulation ($P = 0.0065$). Comparing tumors and corresponding normal lung tissue, we confirmed HOXB2 up-regulated lesions to have much higher HOXB2 expression than the corresponding normal tissue.

In conclusion

Recent studies support the hypothesis that metastatic potential is acquired early in tumorigenesis and that the majority of tumor cells have the potential to metastasize. Although gene expression profiles that can classify cancer patients according to the risk of recurrence have been found in many studies, most of these were retrospective. Very recently, by gene expression profiling, Potti et al. [9] proposed a "lung metagene model" that could identify individuals at increased risk for disease recurrence with stage IA NSCLC. They are now planning to use this for a prospective randomized clinical trial. In the future, more emphasis needs to be placed on translational research to enable basic research findings to be applied in the clinic.

References

1. Brundage MD, Davies D, Mackillop WJ (2002) Prognostic factors in non-small cell lung cancer: a decade of progress. Chest 122(3):1037–1057. doi:10.1378/chest.122.3.1037
2. Miyoshi T, Satoh Y, Okumura S et al (2003) Early-stage lung adenocarcinomas with a micropapillary pattern, a distinct pathologic marker for a significantly poor prognosis. Am J Surg Pathol 27(1):101–109. doi:10.1097/00000478-200301000-00011
3. Inamura K, Shimoji T, Ninomiya H et al (2007) A metastatic signature in entire lung adenocarcinomas irrespective of morphological heterogeneity. Hum Pathol 38(5):702–709. doi:10.1016/j.humpath.2006.11.019
4. Garber ME, Troyanskaya OG, Schluens K et al (2001) Diversity of gene expression in adenocarcinoma of the lung. Proc Natl Acad Sci USA 98(24):13784–13789. doi:10.1073/pnas.241500798
5. Bhattacharjee A, Richards WG, Staunton J et al (2001) Classification of human lung carcinomas by mRNA expression profiling reveals distinct adenocarcinoma subclasses. Proc Natl Acad Sci USA 98(24):13790–13795. doi:10.1073/pnas.191502998
6. Beer DG, Kardia SL, Huang CC et al (2002) Gene-expression profiles predict survival of patients with lung adenocarcinoma. Nat Med 8(8):816–824
7. Ramaswamy S, Ross KN, Lander ES et al (2003) A molecular signature of metastasis in primary solid tumors. Nat Genet 33(1):49–54. doi:10.1038/ng1060
8. Liotta LA, Kohn EC (2003) Cancer's deadly signature. Nat Genet 33(1):10–11. doi:10.1038/ng0103-10
9. Potti A, Mukherjee S, Petersen R et al (2006) A genomic strategy to refine prognosis in early-stage non-small-cell lung cancer. N Engl J Med 355(6):570–580. doi:10.1056/NEJMoa060467
10. Sun Z, Aubry MC, Deschamps C et al (2006) Histologic grade is an independent prognostic factor for survival in non-small cell lung cancer: an analysis of 5018 hospital- and 712 population-based cases. J Thoracic Cardiovasc Surg 131(5):1014–1020. doi:10.1016/j.jtcvs.2005.12.057
11. Inamura K, Fujiwara T, Hoshida Y et al (2005) Two subclasses of lung squamous cell carcinoma with different gene expression profiles and prognosis identified by hierarchical clustering and non-negative matrix factorization. Oncogene 24(47):7105–7113. doi:10.1038/sj.onc.1208858
12. Brunet JP, Tamayo P, Golub TR et al (2004) Metagenes and molecular pattern discovery using matrix factorization. Proc Natl Acad Sci USA 101(12):4164–4169. doi:10.1073/pnas.0308531101
13. Travis WD, Brambilla E, Muller-Hermelink HK, Harris CC (2004) World health organization classification of tumours: pathology and genetics of tumours of the lung, pleural, thymus and heart. Springer, Berlin
14. Jones MH, Virtanen C, Honjoh D et al (2004) Two prognostically significant subtypes of high-grade lung neuroendocrine tumours independent of small-cell and large-cell neuroendocrine carcinomas identified by gene expression profiles. Lancet 363(9411):775–781. doi:10.1016/S0140-6736(04)15693-6
15. Virtanen C, Ishikawa Y, Honjoh D et al (2002) Integrated classification of lung tumors and cell lines by expression profiling.